

Polarizing Properties of Functional Optical Films Based on Lyotropic Chromonic Liquid Crystals

O. P. Boiko
R. M. Vasyuta
V. G. Nazarenko
V. M. Pergamenshchik

Institute of Physics NAS Ukraine, Kyiv, Ukraine

Yu. A. Nastishin

Institute of Physical Optics, Ministry of Education Science of Ukraine,
Lviv, Ukraine

O. D. Lavrentovich

Liquid Crystal Institute & Chemical Physics Interdisciplinary Program,
Kent State University, USA

We report results of the optical characterization of dried thin films obtained from the well-aligned nematic phase of a lyotropic chromonic liquid crystal (LCLC) by two different deposition techniques. The first one, the electrostatic layer-by-layer deposition technique, was used to prepare aligned LCLC films of a nanometer thickness in the form of a monomolecular layer and multi-layered stack. The second technique is the direct deposition technique. The films' optical characteristics such as dispersion of the light absorption indices, birefringence, polarizing efficiency, contrast ratio, transmittance of unpolarized light, were measured and compared with the correspondent characteristics of a cell filled with nematic solution of the same LCLC material.

Keywords: lyotropic chromonic liquid crystal; nano-architecture; self-assemble

INTRODUCTION

Progress in optoelectronics is highly dependent on the development of new reliable low-cost technologies and materials. New materials for

This work was supported by NAS Ukraine grant #1.4.1B/69, CRDF Grant #UK-P1-2617-KV-04, grant for young scientists from President of Ukraine (grant #F11/4-2006) and by Ministry of Education and Science of Ukraine (grant #0106U000617).

Address correspondence to O. P. Boiko, Institute of Physics NASU, 46, Nauky Ave., Kyiv, Ukraine. E-mail: boiko@iop.kiev.ua

functional integral optical films are in great demand. Recently a new class of highly perspective optical materials, lyotropic chromonic liquid crystals (LCLCs), has been intensively studied. LCLCs are obtained from aqueous solutions of dyes: molecules of some dyes aggregate into supramolecular units whose orientational order gives rise to different LC phases (for review, see [1]). The LCLCs can be employed as optical elements for display application in the form of: 1) nematic solution, 2) dried thin film, or 3) nano-film deposited on a transparent solid substrate. The main feature allowing for these applications is the liquid crystalline order: a nematic LCLC can be uniformly aligned and used as an optically birefringent or/and dichroic film. Furthermore, when water evaporates, the resulting dry film still preserves the orientational order and thus anisotropic optical properties. A preserved in-plane long-range orientational order has been demonstrated not only for dried films of a micron thickness, but also for nano-films comprised of just one or a few stacked LCLC monolayers fabricated using the electrostatic layer-by-layer deposition technique [2,3].

Because of the order inherited from the nematic solution, dried LCLC films exhibit a significant anisotropy of light absorption which makes them very attractive for the replacement of the ordinary iodine-based external polarizers in the liquid crystal display production [4–11]. Moreover, dried LCLC films can serve not only as a polarizing film, but also as an alignment layer for the thermotropic liquid crystals [11]. This opens a possibility of development of inexpensive plastic LC displays by placing the polarizing alignment layer of dried LCLC film inside the display. In principle, this scheme can allow one to use a plastic substrate instead of a glass one, as the non-zero birefringence of the plastic does not interfere with the optical performance of the display.

In this article we have performed the optical characterization of dried LCLC films, obtained by two different deposition techniques. The first technique, which is used to prepare aligned LCLC films of a nanometer thickness in the form of monomolecular layer and multi-layered stacks, is the electrostatic layer-by-layer deposition (LLD) from the mesomorphic state of the LCLC [2,3,6]. The assembled dried films demonstrate a long-range orientational order as evidenced by the measurements of absorption as a function of the angle between the deposition direction and polarization of probing light. The second technique is the direct deposition (DD) technique. We report the results of the optical characterization of the solid films, made by these techniques, and compare their optical characteristics.

EXPERIMENTAL

Materials

We work with a dye chromonic material called Blue 27 (6,15-disulfonicacid-7,16-dichloro-indanthrone diammonium salt) obtained from Optiva (CA, USA). Blue 27 is a derivative of indanthrone and absorbs light in the visible light wavelength range. When Blue 27 is dissolved in water the ionic group NH_4^+ leaves the molecule and the ionic residue becomes negatively charged (Fig. 1a). The ionic residues are stacked face-to-face and form rod like aggregates. At room temperature a 4.5% (by weight) water solution of this material forms a nematic phase.

Sample Preparation of Liquid Crystal Cells

Glass substrates, washed in an ultrasonic bath with Alconox detergent for 10 minutes at 60°C and then dried, were covered by a spincoater at 1500 rpm from 3% solution of polymer SE-7511 (Nissan Chemical, Japan) dissolved in Nissan 26 solvent. After one hour baking at 180°C the polymer covered substrates have been unidirectionally rubbed 3 times with an aluminum block wrapped in felt. The cells assembled with the two identical polymer coated substrates, separated by two Mylar strips, were filled with 4.5% water solution of Blue 27. Filling of the cell was performed along the rubbing direction at temperatures of about 10°C higher than the temperature of the phase transition to the isotropic phase ($T \geq 40^\circ\text{C}$) by the pressure gradient

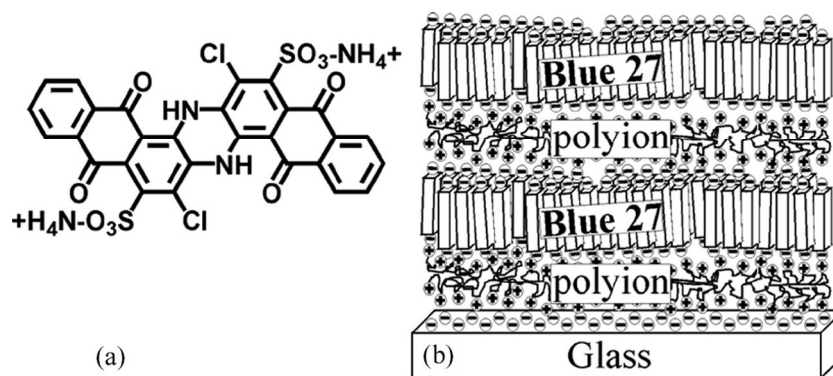


FIGURE 1 Chemical structure of Blue 27 (a) and the structure of a chromonic (Blue 27) film obtained by the LLD technique (b).

from a vacuum pump connected to one of the open sides of the cell through the rubber pipes. Polarizing microscopy examination of the cells reveals a uniform planar orientation of the nematic director.

Layer-by-Layer Deposition Technique

The glass substrates were washed in an ultrasonic bath with a soap detergent, then rinsed in distilled water and dipped into a bath with the glass etching solution (mixture of 5% KOH water solution and isopropanol). After one hour the substrates were removed from the etching solution, rinsed under distilled water and dried. Such cleaning procedure is known to make the surface negatively charged. To reverse the charge of the substrate we cover it by solution of the polymer PDDA (polydiallyldimethylammonium chloride) and let it dry. Because the polymer residuals dissolved in water have positive charge, they are electrostatically adsorbed on the negatively charged glass substrate, and after rinsing the substrate in distilled water the substrate becomes covered by a positively charged PDDA polymer monolayer. Unidirectionally spreading the chromonematic solution on such a substrate, we form a nematic layer with the director parallel to the shearing direction. After drying, the substrates are rinsed with water and the deposited dye material is washed out except an oriented monolayer of the LCLC aggregates. The chromonic molecules are electrostatically adsorbed to the PDDA polymer layer and cannot be washed out. Repeating the deposition procedure for PDDA followed by the deposition of the chromonic monolayers allows one to obtain a solid anisotropic chromonic film with the structure schematically shown in Figure 1b.

Direct Deposition Technique

Glass substrates, washed and cleaned as described above, were covered with a LCLC layer unidirectionally spreading it with a blade. After drying, a texture of the film viewed under the polarization microscopy indicates that the nematic director is on average oriented along the spreading direction. We have measured $k_{\perp} \approx 32000$ (1/cm) for a B27 multilayered stack and used this value to determine the thickness of the film obtained by the direct deposition technique. We found it to be 850 nm.

Optical Characterization Procedure

Optical characteristics. Blue 27 is a light absorbing material. The transmitted intensity for an absorbing crystal plate with its optical

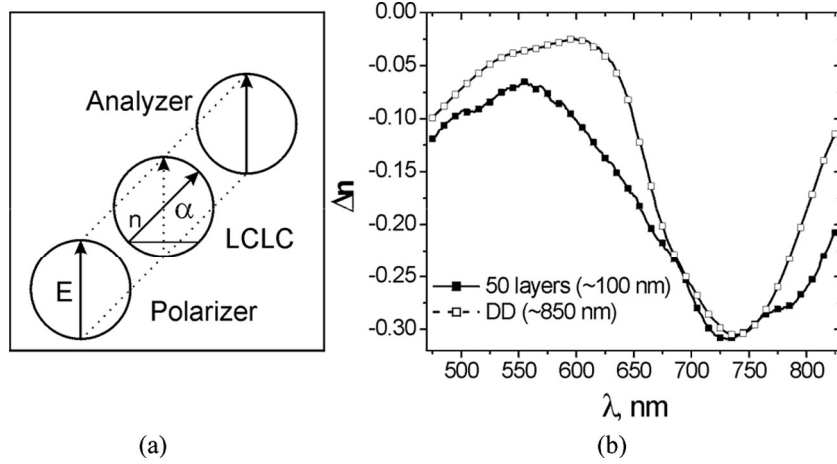


FIGURE 2 The orientation of the nematic director in the chromonic dried film with respect to the parallel polarizers (a) and dispersion of the birefringence for two Blue 27 films: 850 nm thick DD (open squares) and 50 monolayers (solid squares) obtained with the LLD technique (b).

axis oriented at the angle α with respect to two parallel polarizers (see Fig. 2a) can be presented [15]:

$$T = \left(T_{\parallel} \cos^4 \alpha + T_{\perp} \sin^4 \alpha + \frac{\sqrt{T_{\parallel} T_{\perp}}}{2} \cos \Delta \varphi \sin^2 2\alpha \right) \quad (1)$$

where $\Delta \varphi = 2\pi \Delta n d / \lambda$ is the optical phase path, $T_{\parallel} = \exp(-4\pi k_{\parallel} d / \lambda)$ and $T_{\perp} = \exp(-4\pi k_{\perp} d / \lambda)$ are the transmittances for $\alpha = 0$ and $\alpha = 90^\circ$, respectively.

We measured T_{\parallel} , T_{\perp} and calculated the contrast ratio (or extinction ratio) of a polarizer $T_{\perp} / T_{\parallel}$, unpolarized light transmittance of a single polarizer $T = 1/2(T_{\parallel} + T_{\perp})$ and polarizer efficiency

$$P_{\text{eff}} = \frac{T_{\parallel} - T_{\perp}}{T_{\parallel} + T_{\perp}} \times 100\% \quad (2)$$

The transmission spectra $T_{\parallel}(\lambda)$ and $T_{\perp}(\lambda)$ were used to determine the absorption indices k_{\parallel} and k_{\perp} for the light with polarization parallel and perpendicular to the director, respectively.

To determine birefringence Δn from the value $\Delta \varphi$, one needs an additional measurement at an angle different from 0 and 90° . As follows from Eq. (1), the best accuracy is achieved for $\alpha = 45^\circ$. We calculated $\Delta \varphi$ and thus Δn from Eq. (1) using measured transmittance

T_{45} at $\alpha = 45^\circ$ which gives

$$\cos \Delta\varphi = \frac{4T_{45} - (T_{\parallel} + T_{\perp})}{2\sqrt{T_{\parallel}T_{\perp}}}. \quad (3)$$

The expressions above for $T_{\parallel}(\lambda)$ and $T_{\perp}(\lambda)$ and $\cos \Delta\varphi$ allow one to simultaneously measure the absorption, absorption anisotropy and birefringence.

Order parameter. The dimensionality of the order parameter of the film is a delicate issue. Although apparently the DD films seem to be rather of 3D nature while the LLD films seem to be rather 2D, it is difficult to qualify them as being purely either 3D or 2D. In LLD films due to the electrostatic adsorption the dye residues are expected to be strongly fixed at the substrate surface so that the charged groups are in contact with the substrate surface. Therefore, as the long axes of the constituent dye molecules make fixed angle with the aggregate axis, one can imagine that the orientations of the molecular axes and the aggregates' long axes are fixed with respect to the film normal. In this ideal limiting case, the orientational distribution of the dye molecules and aggregates within the film is indeed 2D: it depends on the angle θ that aggregates' long axes make in the monolayer plane with the optical axis (i.e., with the film director which is supposed to be along the shear direction). This 2D order can be fully described by coefficients of the cosine Fourier expansion of the distribution function, the coefficient of $\cos 2\theta$ being the order parameter S_{2D} , see Appendix. There is no guaranty, however, that the long axes of both aggregates and constituent molecules are locked in the plane of the LLD film. Indeed, in general, the electrostatic interaction cannot rigidly fix the aggregate orientation, the surface normal gives just a preferred direction additional to the shear direction, and the order is biaxial. In the limiting case when the interaction favoring the anisotropy along the film normal is weak, the order is 3D uniaxial with the single symmetry axis given by the shear direction, and can be described by the standard 3D order parameter S_{3D} which shows the fraction of the second Legendre polynomial in the expansion of the orientational distribution function. Similar arguments apply to the DD films. Therefore, to avoid the necessity to determine the biaxial order of the films (the task to deserve an individual study) and to make possible comparison of the degrees of their ordering, it is logical to characterize the orientational order within the LLD and DD films by the both order parameters S_{2D} and S_{3D} . Such an approach is particularly justified because both S_{2D} and S_{3D} are calculated from the same experimental data for the dichroic ratio N . If the light absorbing dipole moment of the molecule

is at an angle β with respect to the long axis of the aggregate, the 3D and 2D scalar order parameters can be calculated from the dichroic ratio $N = \ln T_{\parallel} / \ln T_{\perp}$ as follows (see Appendix):

$$S_{3D} = \frac{N - 1}{(N + 2)(1 - 3/2 \sin^2 \beta)}, \quad (4)$$

$$S_{2D} = \frac{N - 1}{2(N + 1) \cos 2\beta}. \quad (5)$$

For Blue 27, (A9) $\beta = \pi/4$ [15] and we have:

$$S_{3D} = \frac{1 - N}{1 + \frac{1}{2}N}; \quad (6)$$

$$S_{2D} = \frac{1}{2} \cdot \frac{1 - N}{N + 1}. \quad (7)$$

RESULTS AND DISCUSSION

From the measured transmission coefficients T_{\parallel} , T_{\perp} , and T_{45} described above we have calculated the birefringence Δn . The results of the dispersion of the birefringence for 850 nm thick DD film are shown in Figure 2b. A possible contribution of the polymer layers to the measured value of the birefringence is not separated here from the birefringence of the chromonic layers. However, the small difference between the two curves in Figure 2b corresponding to the birefringence of the DD and LLD films is of order of the measurement accuracy, indicating that the contribution from the polymer is small and hence the main contribution to the measured Δn value comes from the birefringence of the chromonic layers. For comparison, Figure 3a shows the dispersion of the birefringence measured for the 4.5% Blue 27 solution. For Blue 27 the shape of the dispersion curve is anomalous. The anomaly is related to the presence of the absorption band (Fig. 3a) with the absorption maximum at $\lambda \approx 640$ nm. The absorption indices for both types of the films are shown in Figure 4. For comparison Figure 3b shows the dispersion of the absorption indices for 4.5% Blue 27 nematic cell. The absorption indices for the solution are about 20 times lower than those for the solid films. The absorption indices k_{\perp} for the both type films coincide while k_{\parallel} for the LLD film is higher than for the DD film. The latter implies that the order parameter of the LLD film is lower than that for the DD film.

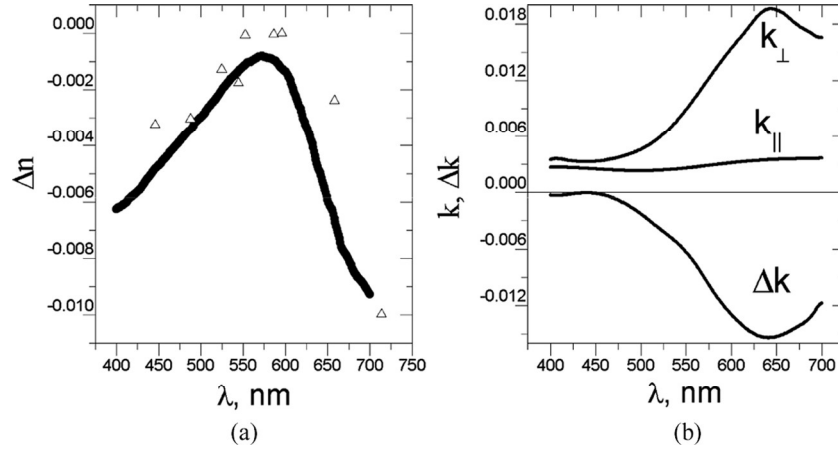


FIGURE 3 Dispersion of the birefringence (a) and dispersion of the absorption indices for the 4.5% Blue 27 in a water solution (b).

Using experimental values of T_{\parallel} and T_{\perp} , we have calculated the scalar order parameters of the prepared films, Figure 5. Comparing the ordering in the films of different types and in the liquid crystal cell, one has to keep in mind that the order parameters S_{3D} and S_{2D} differ by their definitions and by their values for the same value of N , Eqs. (2), (3). Indeed, the maximum possible value for S_{3D} is 1 whereas for

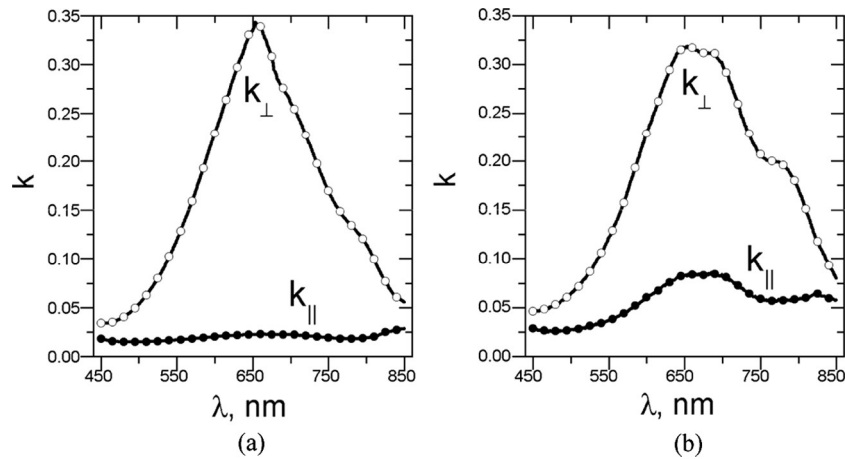


FIGURE 4 Dispersion of the absorption indices for directly deposited (a) and electrostatically deposited films (b) as a function of the wavelength.

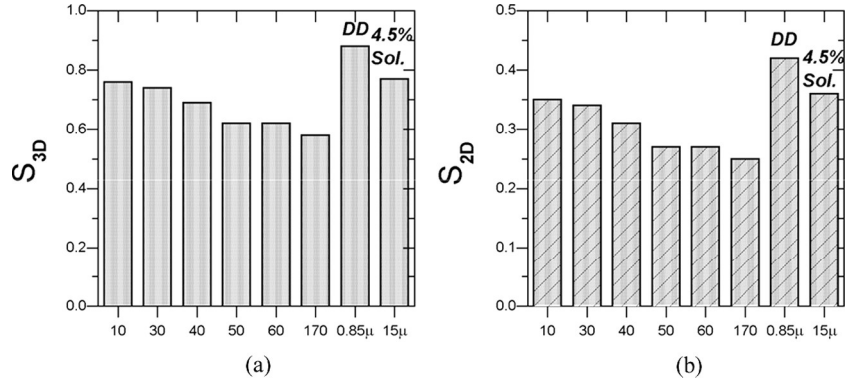


FIGURE 5 Scalar order parameters S_{2D} (a) and S_{3D} (b) for LLD films with different number of layers (one layer is 1.7 nm thick), for the DD film of the thickness 850 nm and for the nematic solution (4.5%) in the cell of 15 μm in thickness.

S_{2D} it is 0.5. Therefore, a meaningful comparison can be made only between like order parameters of different films. Figures. 5a,b shows the plots for S_{3D} and S_{2D} , respectively.

The bars in Figures 5a,b marked with the number of layers correspond to the LLD films, the last two bars on the right sides of the plots represent, respectively, a 850 nm thick DD film and 4.5% nematic solution in the cell with a gap of 15 μm thickness. For DD film, the S_{3D} and S_{2D} order parameters appear to be fairly close to their maximum values (about 0.9 for S_{3D} and almost 0.45 for S_{2D}). For the LLD films there is a clear tendency of a decrease of S_{3D} and S_{2D} order parameters with the increase of the number of deposited layers. This decrease is a result of accumulation of the director misalignment with each next deposited layer which makes the overall distribution about the shear direction broaden. Another clear trend is in the LLD films S_{3D} is lower than the S_{3D} value obtained for the nematic cell (Fig. 5a). For example for 10 layers the value of S_{3D} is 0.72 whereas for the mother nematic solution $S_{3D} = 0.77$.

The results of comparison of the obtained optical characteristics of the nematic cell and the both type films are summarized in Table 1. The last columns in Table 1 display the polarizing efficiency of the films. It is seen that it increases with the increase of the film thickness, but at the same time the increase of the thickness is accompanied by the decrease of the film transmittance T . Direct Deposition technique demonstrates better polarizing properties compared to the LLD technique. This difference can be attributed to the

TABLE 1 Films Parameters at Maximum of Absorbtion and Comparison of the Characteristics of Polarizing Efficiency for DD, LLD and Commercially Available Polarizing Films

No of layers	d, μm	T_{\parallel}	T_{\perp}	T_{\perp}/T_{\parallel}	$T\%$	S_{3D}	S_{2D}	$P_{\text{eff}}, \%$
4.5% solution	15	0.82	0.49	0.60	64	0.77	0.36	25.5
10	0.02	0.97	0.83	0.86	90	0.76	0.35	7.8
30	0.05	0.91	0.61	0.67	76	0.74	0.34	19.5
40	0.07	0.89	0.61	0.68	75	0.69	0.31	18.7
50	0.09	0.79	0.44	0.56	61	0.62	0.27	28.5
60	0.10	0.82	0.50	0.61	66	0.62	0.27	24.5
170	0.29	0.38	0.03	0.08	21	0.58	0.25	84.6
DD	0.85	0.64	.005	0.008	32	0.88	0.42	98.5
Commercially available film*	215				43			99.8

*<http://www.edmundoptics.com/onlinecatalog/displayproduct.cfm?productID=2102&search=1>.

http://www.lgchem.com/en_products/electromaterial/display/polarizer/pola_intro.html.

misalignment in the LLD layer stack described above and absence thereof in thin, but not tethered DD films.

Comparing the polarizing efficiency of our films with the efficiency of a conventional commercially available polarizer (Table 1), one has to notice that our chromonic films are E-polarizers and commercial polarizers referenced in Table 3 are O-polarizers [16,17]. Nevertheless, DD films demonstrate polarizing characteristics which are similar to commercial samples although their thickness is of about 100 times less.

CONCLUSIONS

The comparative optical characterization of the LCLC, namely: 1) nematic cell, 2) DD films and 3) films obtained LLD technique show that the DD films are the most perspective among them. Technological solutions providing a higher scalar order parameter of the films are needed to improve the optical quality of the films.

APPENDIX

Scalar Order Parameter Deduced from the Dichroism

3D scalar order parameter. Consider a nematic phase formed by orientationally ordered rod-like aggregates built of plank-like molecules. The 3D nematic scalar order parameter is the coefficient of

the second order Legendre polynomial in the polynomial expansion of the orientational distribution function which has the form

$$S_{3D} = \frac{1}{2}(3\langle \cos^2 \theta \rangle - 1), \quad (\text{A1})$$

where θ is the angle made by the actual direction of the long axis \vec{A} of a given aggregate and the director \vec{n} , and $\langle \cos^2 \theta \rangle$ denotes the 3D thermodynamic average. The maximum possible value of S_{3D} is 1. For a light absorbing nematic, the value of $\langle \cos^2 \theta \rangle$ can be deduced from the dichroic ratio $N = k_{\parallel}/k_{\perp} = \ln T_{\parallel}/\ln T_{\perp}$. The light absorption coefficients measured for the light polarized, respectively, parallel and perpendicular to the director can be expressed as

$$k_{\parallel} = ad^2 \langle \cos^2 \theta_d \rangle, \quad k_{\perp} = ad^2 \langle \sin^2 \theta_d \rangle \langle \sin^2 \varphi \rangle, \quad (\text{A2})$$

where a is a material constant, \vec{P} is the transition dipole moment, θ_d is the angle between \vec{P} and \vec{n} , φ is the azimuth of \vec{P} with respect to the director, and

$$\langle \sin^2 \varphi \rangle = \frac{1}{2\pi} \int_0^{2\pi} \sin^2 \varphi d\varphi = \frac{1}{2} \quad (\text{A3})$$

The dipole moment \vec{P} of the constituent plank-like molecule makes the fixed angle φ with the aggregate axis \vec{A} . Now the average orientation of the aggregate axis $\langle \cos^2 \theta \rangle$ has to be expressed in terms of the average orientation $\langle \cos^2 \theta_d \rangle$ of the transition dipole entering Eq. (A2). To this end we choose the reference frame connected to the aggregate axis \vec{A} in which this axis is fixed while the director and dipole moment vector spin around. Let the Z-axis be along \vec{A} and the X-Z plane be spanned over the vectors \vec{A} and the instant orientation of \vec{n} , Figure 6 (left side). In this reference frame the dipole moment \vec{P} of the constituent molecule has the azimuth φ with respect to the X-axis. The relation between θ and θ_d is now seen to be of the form

$$\cos \theta_d = \cos \theta \cos \beta + \sin \theta \sin \beta \cos \gamma. \quad (\text{A4})$$

Averaging the square of the relation (A4) over θ and γ , one obtains

$$\langle \cos^2 \theta_d \rangle = \langle \cos^2 \theta \rangle \cos^2 \beta + \frac{1}{2} \langle \sin^2 \theta \rangle \sin^2 \beta \quad (\text{A5})$$

where $\langle \sin^2 \gamma \rangle = 1/2$ (the averaging over the rotation of the X-axis about the Z-axis is trivial as (A5) does not depend on the rotation angle). From this equation one has

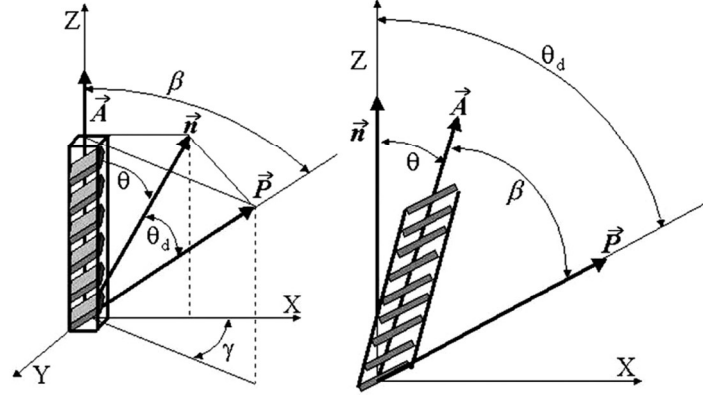


FIGURE 6 To explanation of 3D (left) and 2D (right) scalar order parameters.

$$\langle \cos^2 \theta \rangle = \frac{\langle \cos^2 \theta_d \rangle - (1/2) \sin^2 \beta}{1 - 3/2 \sin^2 \beta}, \quad (\text{A6})$$

From Eqs. (A6) and (A1)–(A3), the 3D scalar order parameter finally obtains in the form

$$S_{3D} = \frac{N - 1}{(N + 2)(1 - (3/2) \sin^2 \beta)} \quad (\text{A7})$$

For $\beta = \frac{\pi}{2}$ we have: $S_{3D}(\pi/2) = \frac{1 - N}{1 + N/2}$ (A8)

2D scalar order parameter. In the 2D case the aggregates are electrostatically adsorbed onto the plane of substrate to which they remain restricted all the time, Figure 6 (right side). The 2D order parameter is the coefficient of $\cos 2\theta$ in the Fourier expansion of the 2D orientational distribution function which has the form

$$S_{2D} = \frac{1}{2} (2 \langle \cos^2 \theta \rangle - 1) \quad (\text{A9})$$

where $\langle \cos^2 \theta \rangle$ stands for the 2D thermodynamical average. In contrast to the 3D order parameter (A1), the maximum possible value of S_{2D} is 1/2. In the 2D case, instead of (A2) one has

$$N = \frac{k_{\parallel}}{k_{\perp}} = \frac{\langle \cos^2 \theta_d \rangle}{\langle \sin^2 \theta_d \rangle}. \quad (\text{A10})$$

As the long molecular axis has two equivalent lateral surfaces, the angle β can take two values, $+\beta$ which is the case shown in Figure 3A, and $-\beta$ in which case the lateral side we see in Figure 3A would be turned to the Figure plane and the vector \vec{P} would be leftward the aggregate axis \vec{A} . The relation $\theta = \theta_d - \beta$ can be converted into the formula

$$\cos^2 \theta_d = \cos^2 \theta \cos 2\beta - (1/2) \sin 2\theta_d \sin 2\beta + \sin^2 \beta. \quad (\text{A11})$$

Averaging (A11) over θ , summing over $\pm\beta$, one has

$$\langle \cos^2 \theta_d \rangle = \langle \cos^2 \theta \rangle \cos^2 \beta + \langle \sin^2 \theta \rangle \sin^2 \beta. \quad (\text{A12})$$

Now from Eqs. (A9), (A10), and (A12) one finally obtains

$$S_{2D} = \frac{N-1}{2(N+1) \cos 2\beta}. \quad (\text{A13})$$

For $\beta = \frac{\pi}{2}$ we find: $S_{2D}(\pi/2) = \frac{1-N}{2(N+1)}. \quad (\text{A14})$

REFERENCES

- [1] Lydon, J. (1998). In: *Handbook of Liquid Crystals*, Demus, D., Goodby, J., Gray, G. W., Spiess, H.-W., & Vill, V. (Eds.), Wiley-VCH: Weinheim, and references therein, Vol. 2B, 981–1007.
- [2] Schneider, T. & Lavrentovich, O. D. (2000). *Langmuir*, 16, 5227; *Alignment of lyotropic chromonic liquid crystals at surfaces as monolayers and multilayered stacks*, US patent #6, 673, 398 (January 6, 2004).
- [3] Schneider, T., Artyushkova, K., Fulghum, J. E., Broadwater, L., Smith, A., & Lavrentovich, O. D. (2005). *Langmuir*, 21, 2300.
- [4] Dreyer, J. F. & Ertel, C. W. (1948). *J. Phys. Colloid Chem.*, 52, 808; Dreyer, J. F. US patent 2,481,830; Dreyer, J. F. US patent 2,544,659, March 13, 1951.
- [5] Mundy, K., Sleep, J. C., & Lydon, J. E. (1995). *Liq. Crystals*, 19, 107.
- [6] Sergan, T., Schneider, T., Kelly, J., & Lavrentovich, O. D. (2000). *Liquid Crystals*, 27, 567.
- [7] Ignatov, L., Lazarev, P. I., Nazarov, V., Ovchinnikova, N., & Paukshto, M. (2002). *Proc. SPIE*, 4807, 177.
- [8] Ignatov, L., Lazarev, P. I., Nazarov, V., & Ovchinnikova, N. (2002). *Proc. SPIE*, 4658, 79.
- [9] Bobrov, Y., Grodsky, A., Ignatov, L., Krivostchepov, A., Nazarov, V., & Remizov, S. (2001). *Proc. SPIE*, 4511, 133.
- [10] Wip, W. C., Kwok, H. S., Kozenkov, V. M., & Chigrinov, V. G. (2001). *Displays*, 22, 27.
- [11] Sergan, T., Schneider, T., Kelly, J., & Lavrentovich, O. (2000). *Liq. Cryst.*, 27, 567.

- [12] Tam-Chang, S.-W., Seo, W., Iverson, I. K., & Casey, S. M. (2003). *Angew. Chem. Int. Ed.*, **42**, 897.
- [13] Boiko, O., Komarov, A., Vasyuta, R., Nazarenko, V., Slominskiy, Yu., & Schneider, T. (2005). *Mol. Cryst. Liq. Cryst.*, **434**, p. 305 [633].
- [14] Advincula, R. C., Fells, E., & Park, M.-K. (2001). *Chem. Mater.*, **13**, 2870.
- [15] Nastishin, Yu. A., Liu, H., Schneider, T., Nazarenko, V., Vasyuta, R., Shiyanovskii, S. V., & Lavrentovich, O. D. (2005). *Phys. Rev. E*, **72**, 041711.
- [16] Lazarev, P. & Paukshto, M. (2001). *Journal of the Society for Information Display*, **9/2**, 101.
- [17] Yeh, P. & Paukshto, M. (2000). *Molecular Materials*, **14**, 1.